Thermal Vacuum Testing of a Helium Loop Heat Pipe for Large Area Cryocooling

Jentung Ku[1] and Franklin Robinson[2]
NASA Goddard Space Flgiht Center, Greenbelt, Maryland, 20771

Future NASA space telescopes and exploration missions require cryocooling of large areas such as optics, detector arrays, and cryogenic propellant tanks. One device that can potentially be used to provide closed-loop cryocooling is the cryogenic loop heat pipe (CLHP). A CLHP has many advantages over other devices in terms of reduced mass, reduced vibration, high reliability, and long life. A helium CLHP has been tested extensively in a thermal vacuum chamber using a cryocooler as the heat sink to characterize its transient and steady performance and to verify its ability to cool large areas or components in the 3K temperature range. The helium CLHP thermal performance test included cool-down from the ambient temperature, startup, capillary limit, heat removal capability, rapid power changes, and long duration steady state operation. The helium CLHP demonstrated robust operation under steady state and transient conditions. The loop could be cooled from the ambient temperature to subcritical temperatures very effectively, and could start successfully by simply applying power to both the capillary pump and the evaporator plate without pre-conditioning. It could adapt to a rapid heat load change and quickly reach a new steady state. Heat removal between 10mW and 140mW was demonstrated, yielding a power turn down ratio of 14. When the CLHP capillary limit was exceeded, the loop could resume its normal function by reducing the power to the capillary pump. Steady state operations up to 17 hours at several heat loads were demonstrated. The ability of the helium CLHP to cool large areas was therefore successfully verified.

Nomenclature

CC = compensation chamber
CLHP = cryogenic loop heat pipe
CTE = coefficient of thermal expansion
GSFC = Goddard Space Flight Center
LHP = loop heat pipe
MLI = multi-layer insulation
NASA = National Aeronautics and Space Administration
NESC = NASA Engineering and Safety Center
SBIR = Small Business Innovation Research
$C_{p,l}$ = specific heat of liquid
$C_{p,v}$ = specific heat of vapor
$\dot{m}$ = mass flow rate of working fluid
Q_{COND} = heat dissipation by condenser
Q_{PUMP} = heat load to capillary pump
Q_{EVAP} = heat load to evaporator
T_{CC} = compensation chamber temperature
T_{COND} = condenser temperature
T_{EVAP} = evaporator temperature
T_{PUMP} = pump temperature
T_{SAT} = saturation temperature
T_{VAPOR} = vapor temperature

[1] Lead Aerospace Engineer, Thermal Engineering Branch, Code 545, Goddard Space Flight Center, Greenbelt, MD.
[2] Aerospace Engineeri, Thermal Engineering Branch, Code 545, Goddard Space Flight Center, Greenbelt, MD.

ΔT_{SUB} = amount of liquid subcooling
ΔT_{SUP} = amount of vapor superheat
η = effectiveness of capillary pump to convert applied heat to mass flow rate
λ = latent heat of vaporization
x = vapor quality
ξ = overall efficiency of CLHP

I. Introduction

CRYOCOOLING of large areas, such as optics, detector arrays, and cryogenic propellant tanks, is required for future space telescopes and exploration missions of the National Aeronautics and Space Administration (NASA). Because loop heat pipes (LHPs) have been used on many orbiting spacecraft in the room temperature range [1-6], one concept for such applications is to use the LHP by extending its operating temperature to the cryogenic temperature range. The cryogenic loop heat pipe (CLHP) has a great potential due to its inherent advantages: 1) long life time because of no liquid boil-off in a closed loop; 2) isolating optics and detectors from the mechanical vibration of the cryopump which is located remotely; and 3) accommodating various geometries of the heat source to be cooled because of small thin-walled flexible lines used in the CLHP.

Under the NASA Small Business Innovation Research (SBIR) program, a helium CLHP was successfully developed in 2007 and demonstrated its feasibility for cryocooling over a large area. Because of schedule and budget constraints under the SBIR, the helium CLHP was tested for limited test runs under transient conditions using a dewar as the heat sink. Through the sponsorship of the Passive Thermal and Propulsion Technical Discipline Teams at the NASA Engineering and Safety Center (NESC), the Goddard Space Flight Center (GSFC) has conducted extensive tests on the existing CLHP to characterize its steady state and transient performance and to verify its ability to cool large areas. The existing CLHP was reconfigured using a cryopump as the heat sink (the same as in flight applications), and tested in a thermal vacuum chamber using neon and helium as working fluids. The thermal performance tests of the CLHP included loop cool-down from the ambient temperature, startup, operation with large power changes (power cycles), evaporator heat removal capability, capillary limit and loop recovery from dry-out, low power operation, and long duration steady state operation.

Testing of the CLHP with neon as the working fluid in the temperature range of 30K to 40K was reported earlier [7]. This paper summarizes the experimental results of the CLHP test using helium as the working fluid for temperatures between 3.2K and 4.0K, and is organized in the following order: 1) theoretical background, 2) test article and test setup; 3) tests performed and experimental results; and 4) summary and conclusions.

II. Theoretical Background

Figure 1 shows the schematic of a typical LHP, which consists of an evaporator (capillary pump) with an integral reservoir (also known as the compensation chamber or CC), a condenser, a vapor line and a liquid line. The evaporator contains a primary wick which sustains the pressure drop induced by the fluid flow around the loop, and a secondary wick which connects the evaporator to the reservoir. The rest of the loop is made of smooth tubes. More details about the LHP and its operating principles can be found in the literature [8-11].

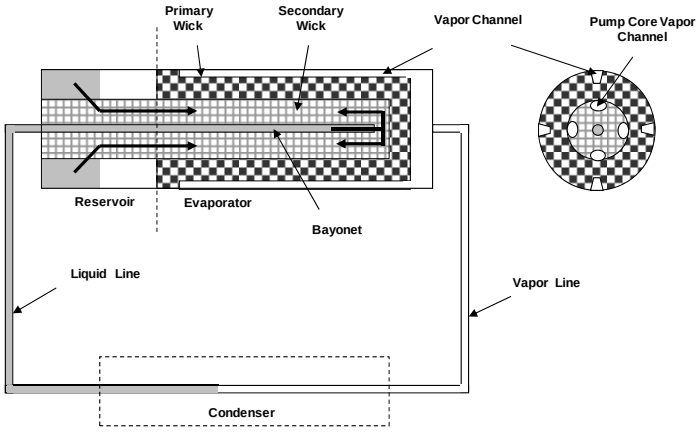

Figure1. Schematic of a Typical LHP

LHPs have been used on many NASA spacecraft and communications satellites in the ambient temperature range [1-6]. Extending the application of the existing LHP to cryogenic temperatures faces several challenges [12-14], including: 1) containment of high internal pressures; 2) loop startup from an initially supercritical condition; 3) a mismatch in coefficients of thermal expansion (CTE) between the primary wick and the evaporator shell; and 4) collecting heat from a large area.

The challenges of pressure containment and startup can be overcome by using a pressure reduction reservoir (also known as the "hot" reservoir) and the issue of CTE mismatch can be resolved by using the same

material for both the primary wick and evaporator shell [12-14]. Cooling of large areas and then delivering the acquired heat to a cryocooler cold finger with a small interface area for rejection requires some basic change in the LHP configuration because it is opposite to the function of a traditional LHP which acquires waste heat from a small area, transports it to a heat sink, and then distributes it over a large area for ultimate heat rejection.

Under the NASA SBIR Program, TTH Research, Inc. developed the concept of a CLHP/cryocooler system which can be used for large-area cryocooling, as shown in Figure 2 [14]. Main features of this design are: 1) The capillary pump (i.e. the evaporator in the traditional LHP) is used solely to generate a fluid flow in the loop and electrical heaters attached to the capillary pump provide the necessary power for the fluid circulation. 2) The fluid in the transport line passes through a cold plate attached to a cryocooler and the heat source alternately. Thus, vapor generated in the capillary pump will condense into liquid as it passes through the cold plate, and liquid will vaporize as it passes through the heat source. 3) The amount of heat that can be removed by the evaporator from the heat source is a function of the heat applied to the capillary pump and the number of passes that the fluid flows through the cold plate and the heat source. 4) The maximum amount of heat that can be applied to the capillary pump is determined by the heat transport capability of the capillary pump. 5) A hot reservoir (not shown in Figure 2) is connected to the loop on the last leg of the evaporator line before it enters the reservoir.

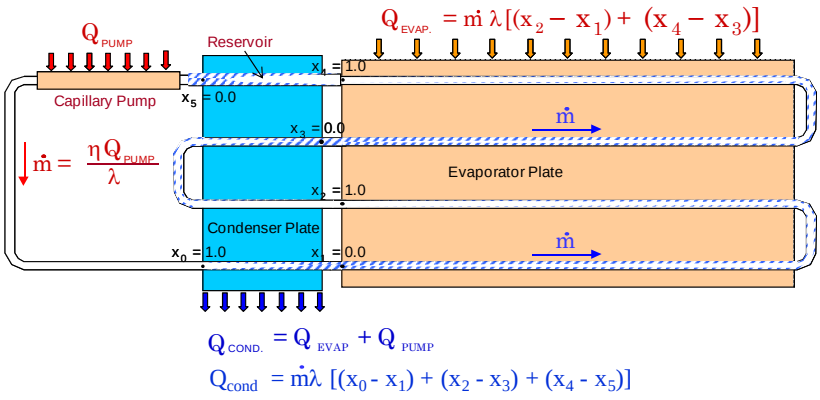

Figure 2. CLHP/Cryocooler System Concept

The mass flow rate in the loop, $\dot{m}$, is proportional to the heater power applied to the capillary pump:

$$\dot{m} = \eta Q_{PUMP}/\lambda \qquad (1)$$

If the heat leak from the capillary pump to the CC is zero, η is equal to 1. Otherwise, η is less than 1. The heat acquired by the fluid flow in the evaporator is:

$$Q_{EVAP} = \dot{m}\lambda \sum_{i=1}^{N}(x_{2i} - x_{2i-1}) \qquad (2)$$

From Eq. (1), Eq. (2) becomes:

$$Q_{EVAP} = \eta Q_{PUMP} \sum_{i=1}^{N}(x_{2i} - x_{2i-1}) \qquad (3)$$

The overall efficiency of the CLHP/cryocooler system, where the CLHP makes N loopbacks between the heat source and the cryocooler can be defined as:

$$\xi = \frac{Q_{EVAP}}{Q_{PUMP}} = \eta \sum_{i=1}^{N}(x_{2i} - x_{2i-1}) \qquad (4)$$

The operation of the CLHP shown in Figure 2 for large area cryocooling is in many ways different from that of the traditional LHP shown in Figure 1. First, an external power to the capillary pump is required in order to circulate the fluid around the loop. Second, the fluid flow runs alternately between the condenser and the evaporator in order to remove heat from the evaporator and reject it to the condenser. Third, the CC serves as a condenser to remove heat absorbed by the last leg of the evaporator in addition to its traditional function of managing the liquid in the loop and control the loop operating temperature. There is no liquid return line between the condenser and the CC. Fourth, there is a mass exchange between the hot reservoir and the loop as the operating condition changes. This means that the fluid inventory in the CLHP is constantly changing during the loop transient operation although the total fluid mass in the CLHP and hot reservoir is fixed.

III. Test Article and Test Set-up

Figure 3 shows a picture of the CLHP delivered by TTH Research, Inc. in 2007. The silicone diode temperature sensors were installed after delivery for this test program. The CLHP consisted of a capillary pump, a reservoir (CC), a vapor line, a condenser and an evaporator. All the CLHP components were made of stainless steel to mitigate the potential issue of a CTE mismatch. Table 1 summarizes major design parameters of the CLHP. A portion of the transport line was embedded into the condenser plate connected to the cryocooler for vapor condensation, while another portion was embedded into the evaporator plate attached to the heat source for liquid evaporation. Both the condenser and evaporator plates were made of copper. The CC was soldered to the condenser plate to provide a direct thermal path to the cryocooler. The CC hence also served as a condenser. A copper saddle with two embedded cartridge heaters was attached to the capillary pump to provide the necessary power for the flow circulation.

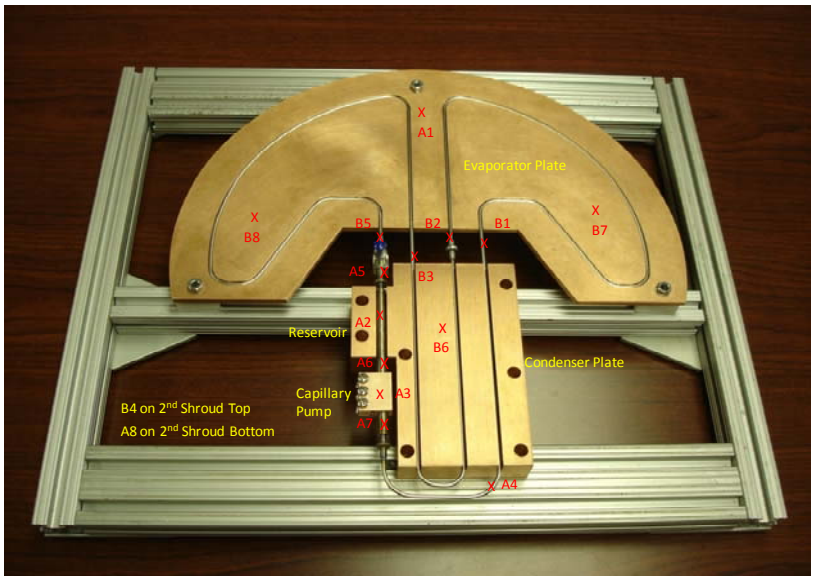

Figure 3. The Helium CLHP on a Support Fixture

Table 1. Major Design Parameters of CLHP

Item	Material	Dimensions/Properties
Capillary Pump	Stainless Steel	6.35mm O.D. x 5.08mm I.D. x 38.1 mm L
Primary Wick	Stainless Steel	5.08mm O.D. x 2.39mm I.D.; pore radius = 1.32 μm; porosity = 0.4, permeability = 1.5 x 10^{-14} m^2
Compensation Chamber	Stainless Steel	6.35mm O.D. x 5.08 mm I.D. x 43.18mm L
Vapor Line	Stainless Steel	2.38mm O.D. x 1.57mm I.D. x 100.3mm L
Condenser Line	Stainless Steel	2.38mm O.D. x 1.57mm I.D. x 448.6mm L
Evaporator Line	Stainless Steel	2.38mm O.D. x 1.57mm I.D. x 1000.8mm L
Condenser Plate	Copper	139.7mm x 88.9mm x 25.4mm thick
Evaporator Plate	Copper	2.19 x 10^4 mm^2 x 4.8mm thick
Hot Reservoir	Stainless Steel	Internal volume = 1.0x10^{-3} m^3
Line between CLHP and Hot Reservoir	Stainless Steel	1.59mm O.D. x 0.254mm wall x 1030mm L
Working Fluid	Helium	Fluid inventory: 0.436 gram

Not shown in Figure 3 was a hot reservoir that was made of stainless steel with an internal volume of 1000cc and plumbed to the test loop. The hot reservoir served two purposes: (i) to provide an expansion volume for the fluid at the system maximum temperature so that the loop pressure could be kept at a manageable level; and (ii) to lower the system pressure below the fluid critical pressure prior to the loop startup. The hot reservoir needs to be placed in a hot environment and thermally isolated from the loop in order to be effective. Accordingly, a 1.59 mm O.D. x 0.254mm wall x 1030 mm L stainless steel line was used to connect the hot reservoir to the CLHP at the location on the last leg of the evaporator line near temperature sensor A5 shown in Figure 3.

The required fluid inventory can be calculated from the volumes of the CLHP components, the hot reservoir and the connecting line between the CLHP and hot reservoir, and their respective temperatures during the CLHP operation. The fluid inventory is then converted into the charge pressure at the ambient temperature of 298K. Volumes of the CLHP, hot reservoir, and connecting line are 4.86cc, 1000cc, and 0.93cc, respectively. Based on the intended CLHP operating temperatures (3.2K to 4.0K), the required charge pressure was 230 KPa (33.4 psi). From

past experience with traditional LHPs, the CLHP was charged with 266 Kpa (38.6psi or 0.436 gram) of helium, which was about 15% higher than theoretically required Charging was performed by first evacuating the entire CLHP and hot reservoir and then introducing the desired amount of helium. . Test results showed that the loop worked quite well with this amount of charge.

Testing of the CLHP was conducted using a 914.4-mm diameter Dynavac chamber shown in Figure 4. The Dynavac chamber is a cryopumped chamber with an LN2 shroud measuring 812.8 mm in diameter and 1371.6mm in height. The shroud extension for the Dynavac chamber housed the two-stage Sumitomo cryocooler, with a secondary stage capable of 1.5 W of cooling at 4.2K and 5 W of cooling at 6.1K. The first stage of the cryocooler is capable of 20 W of cooling at 36.9K and 60 W at 62.3K.

The CLHP was placed inside a secondary shroud which was in turn surrounded by the Dynavac chamber LN2 primary shroud as shown in Figure 5(a). Figure 5(b) depicts a side view (viewed from the left) showing an L-shaped copper bracket connecting the CLHP condenser plate to the cold finger of the cryocooler second stage. The secondary shroud minimizes radiation heat exchange between the CLHP and the primary shroud which has a minimum temperature of 80 K when cooled by liquid nitrogen.

Figure 4. Dynavac Chamber with Shroud Extension Installed

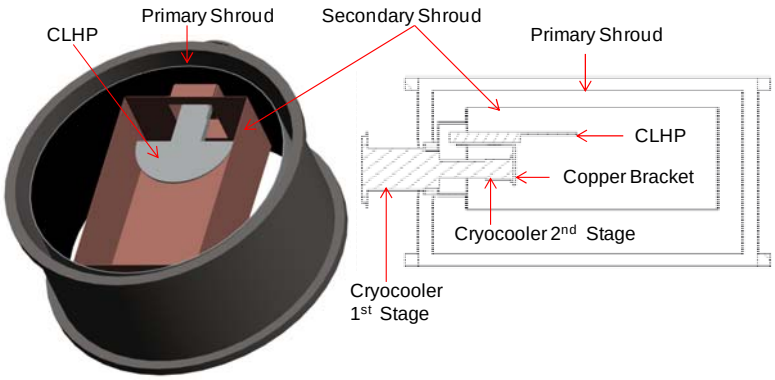

(a) (b)

Figure 5. (a) CLHP Inside a Secondary Shroud Which Was Surrounded by Primary Shroud of Thermal Vacuum Chamber; (b) Side View (Left View) – Copper Bracket Connecting CLHP Condenser to 2nd Stage of Crycooler

The CLHP was instrumented with 14 Lake Shore DT-670 silicon diodes to measure the temperatures as shown in Figure 3. One additional silicon diode was installed on the top surface and another on one side surface of the secondary shroud, respectively. The secondary shroud was cooled by the cryocooler first stage to a pre-determined temperature. A number of thermocouples were also attached to the Dynavac chamber to monitor its temperatures. An absolute pressure transducer with a range of 0 - 344.7 kPa (0-50 psia) and an accuracy of 0.5% is installed in the test loop to keep track of the system pressure. There is a one-to-one relationship between the helium pressure and its corresponding saturation temperature, and such a relationship was coded into the LabView software used to control and monitor the test. Thus, the loop saturation temperature could be determined from the measured pressure at any given time.

Figure 6 shows a picture of the CLHP placed inside the thermal vacuum chamber before it was covered with MLI and before the secondary shroud was closed with its upper plate. A stainless rod was placed across the sides of the secondary

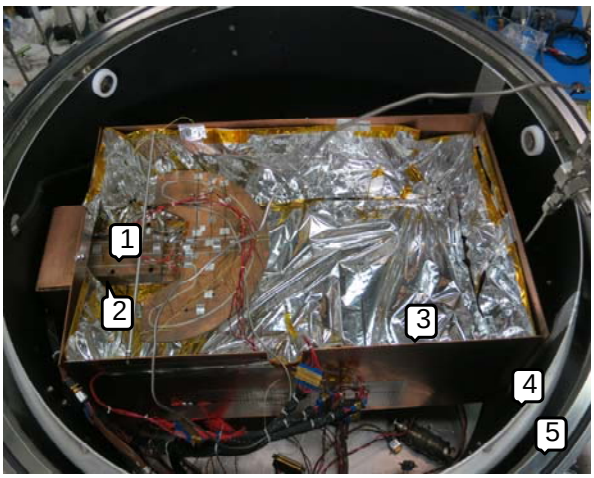

Figure 6. CLHP Inside Dynavac Chamber. 1-CLHP; 2-Cryocooler Mounting Bracket; 3-Secondary Shroud; 4-Primary Shroud; 5-Dynavac Chamber

shroud, and Kevlar strings connected to the two ends of the rod were holding the CLHP in a horizontal position. This particular measure was taken to minimize the parasitic heat gains to the CLHP.

Two embedded cartridge heaters were attached to the capillary pump to provide the power that was necessary to maintain the flow circulation, and two Kapton-backed heaters were bonded to the evaporator surface to provide the heat load. In addition, three Kapton-backed heaters were bonded to the top and side surfaces of the secondary shroud. Three power supplies independently regulated the power inputs to the capillary pump, evaporator plate, and secondary shroud surfaces. The entire CLHP was thermally insulated from the secondary shroud with 12-layer MLI blankets. The primary shroud temperature was kept around 100K whereas the secondary shroud temperature was maintained between 26K and 45K. Hence, the heat parasitics gained by the test loop was minimal. Accurate assessment of the test loop cooling capacity was therefore possible.

The data acquisition system consisted of a desktop computer, two screen monitors, a data logger, and LabView software. Temperatures from silicon diodes and thermocouples, and powers to the capillary pump, evaporator plate, and secondary shroud surfaces were displayed on the monitors and recorded and stored in the personal computer with a frequency set by the test engineer.

IV. Tests Performed and Test Results

As stated before, the operation of the CLHP for large area cryocooling is in many ways different from that of the traditional LHP. In addition, this CLHP being tested had other special features. First, the evaporator copper plate had an extremely high thermal conductivity at low temperatures. Throughout this test program, all silicon diodes installed on the evaporator plate (A1, B7 and B8) showed a uniform temperature for temperatures below 50K. Thus, the ability to gain insights on the physical processes undergone by the fluid inside the evaporator was lost. For example, the fluid might enter the evaporator as subcooled liquid, vaporize at the saturation temperature, and then exit as superheated vapor. In other words, the fluid inside the same leg of the evaporator line could be in different states, but the temperature sensors on the evaporator copper plate would show a uniform temperature. Hence, locations where the liquid evaporation started and where the vapor became superheated could not be known. Second, the specific heat of copper decreased drastically with a decreasing temperature. Thus, most of the heat load applied to the evaporator was dissipated into the fluid; very little was stored in the evaporator plate. This helped the loop to reach a new steady state quickly when the operating condition changed. Third, the cryocooler had a high cooling capacity. The second stage could remove 1.5W at 4.2K. In all test, the sum of the pump power (Q_{PUMP}) and evaporator power (Q_{EVAP}) was no more than 250 mW. Thus, it was possible that vapor from the capillary pump was completely condensed and become subcooled liquid before entering the evaporator. Likewise, vapor exiting the evaporator could become subcooled liquid in the condenser before entering the next leg of the evaporator.

Test results are presented below. Note that, in all of the following figures, the saturation temperature, T_{SAT}, was calculated from the corresponding measured saturation pressure using polynomial curve fitting of the helium property data. In addition, the symbol in the parenthesis for each curve refers to the temperature sensor number shown in Figure 3.

A. Evaporator Cooldown

When the test first began, all components were at the ambient temperature of 298K. After the cryocooler was turned on, the temperature of the secondary shroud was set to 45K. It was envisioned that, based on the load map provided by the cryocooler vendor, this would optimize the performance of the first and second stages of the cryocooler for the planned CLHP tests.

Figure 7 and Figure 8 depict temperature profiles of CLHP components during cool-down from 298K. As the cold finger temperature dropped, so did temperatures of the condenser plate and the CC which were attached to the cold finger via a copper bracket. The capillary pump temperature also dropped primarily due to heat conduction through the metal, and to some degree due to its internal fluid connection to the CC and condenser plate. After more than 6 hours, the condenser and CC were cooled below the helium critical temperature (~5.2K). Liquid was formed and T_{SAT} dropped to around 5K. The evaporator plate was still above 280K because the only thermal connection between the evaporator plate and the condenser plate was through the small stainless steel lines, which had a very small thermal conductivity that decreased with a decreasing temperature. Note that, unless the loop pressure was below the helium critical pressure, no liquid could be formed even when the temperature was below the helium critical temperature. This is why proper sizing of hot reservoir and proper charging of the fluid are so important for a given CLHP at its intended operating temperature range.

The evaporator temperature decreased from 280K to 154K over a 24-hour period. During this period, attempts were made to accelerate the cooling of the evaporator by applying 10 – 30 mW of heat to the capillary pump to circulate the fluid. It turned out that this effort had little effect on the cooling rate of the evaporator plate because heat conduction from the evaporator plate to the condenser plate through the stainless steel lines was the dominant mechanism of the heat transmission. Only after the evaporator temperature dropped below about 50K, where the specific heat of copper dropped by 7 fold and the thermal conductivity of stainless steel dropped by more than 2 fold, did the circulation of the helium fluid help the cool-down of the evaporator plate. All in all, it took about 68 hours to cool the evaporator plate from 298K to 3.5K.

Figure 8 shows that the evaporator temperature dropped steeply after being cooled below 30K. This was because the specific heat of copper becomes extremely small at low temperatures.

B. Loop Startup

Startup of the traditional LHPs could be difficult and problematic under certain conditions and would require pre-conditioning of the loop to enhance the startup success [15, 16]. In this helium CLHP test program, no preconditioning of the loop was conducted. Moreover, the loop always started successfully if heat loads were applied to both the capillary pump and evaporator plate. On the other hand, the loop might not start if the heat load was applied to the capillary pump alone.

Figure 9 shows loop temperatures during the startup of the CLHP with 20 mW to the capillary pump and 20mW to the evaporator plate. The loop started almost immediately as evidenced by the rise of the vapor temperature to T_{SAT}. During the startup transient, T_{SAT} rose because the CC received additional heat from the evaporator. The loop soon reached a steady state. At a low heat load of 20 mW, T_{EVAP} was only slightly higher than T_{SAT} due a high heat transfer coefficient associated with liquid boiling. The pump temperature, T_{PUMP}, was measured on the outer surface of the pump shell, which was made of stainless steel and had a very low thermal conductivity at low

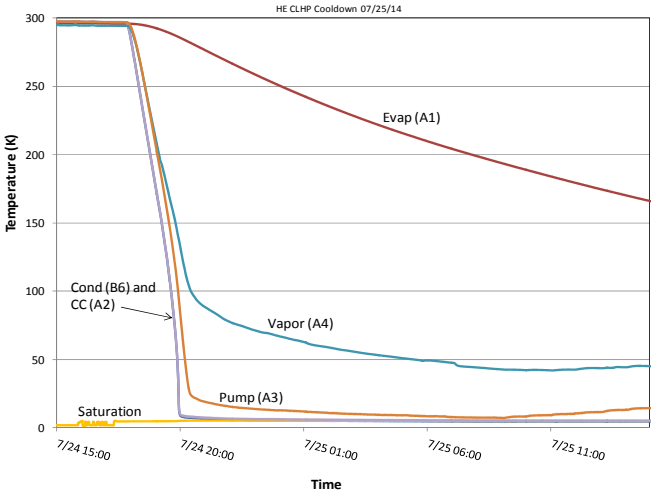

Figure 7. Cool Down of CLHP from Ambient Temperature

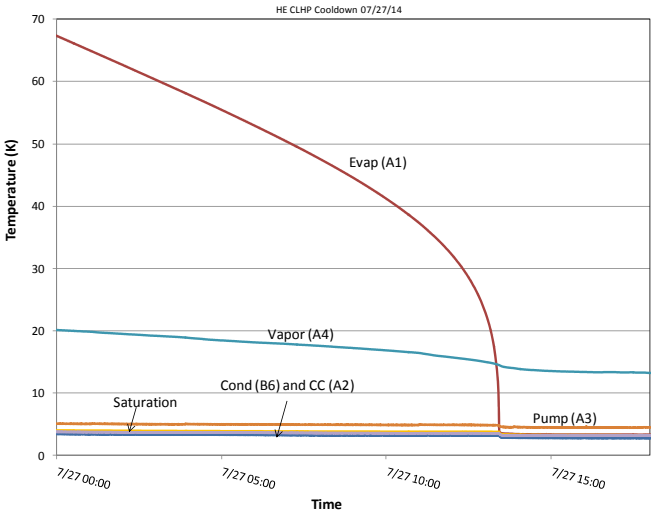

Figure 8. Cool Down of Evaporator

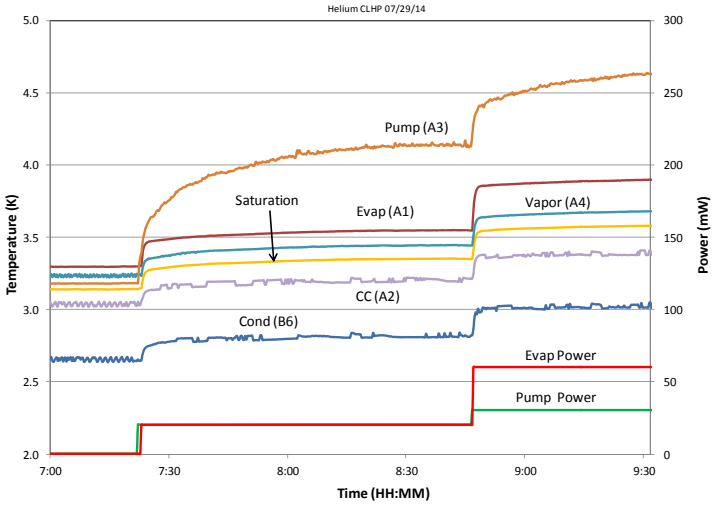

Figure 9. Loop Startup with 20mW/20mW to Pump/Evaporator

temperatures, resulting in a high temperature differential relative to T_{SAT}. The CC temperature was between the calculated loop saturation temperature T_{SAT}.and the condenser temperature. It is lower than the loop saturation temperature because the temperature sensor was installed on the CC itself which was embedded in the saddle connected to the condenser plate. The vapor line temperature (A4) was very close to T_{SAT} at all times, confirming that the T_{SAT} calculated from the measured loop pressure did indicate a reliable loop saturation temperature.

Several other startup tests were conducted with various powers to the capillary pump and evaporator plate. As long as both the pump and evaporator plate received powers, all startup tests were successful. Based on the experience with previous neon loop testing [7], the loop was not expected to start successfully when the heat load was applied to the capillary pump alone. It is postulated that, under this startup condition, the evaporator will be filled with liquid and the capillary pump will not have enough liquid, leading to partial dry-out of the capillary pump.

Figure 10 shows temperature profiles of an attempt to start the loop by applying 30 mW to the capillary pump and no power to the evaporator plate. The flow circulation started immediately after power was applied to the pump. However, T_{PUMP} did not reach a steady state. In fact, T_{PUMP} began to fluctuate after about 20 minutes. As soon as a heat load of 30 mW was applied to the evaporator plate, the loop started successfully and reached a steady state shortly after. This result seemed to confirm the above-mentioned postulate that the evaporator would be filled with liquid without any power to the evaporator and the startup would not be successful. However, in one of the tests, the loop started successfully with 20 mW applied to the pump alone as shown in Figure 11. Apparently, the initial fluid distribution was an important factor. With temperature sensors on the evaporator (A1, B7, B8) showing a uniform temperature, the fluid status inside the evaporator was not known.

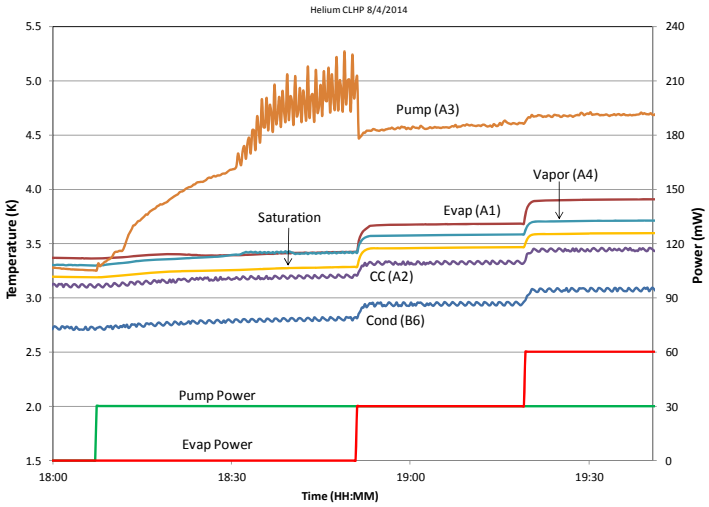

Figure 10. Unsuccessful Startup with Power to Pump Only

C. Power Rampup

Various tests with different combinations of Q_{PUMP}/Q_{EVAP} were performed to characterize the loop performance and to investigate the loop behaviors under steady state and transient conditions. Figure 11 shows the results of a power ramp-up test where Q_{PUMP} and Q_{EVAP} were changed. It is seen that the loop could reach a new steady state very quickly after each power change. In a traditional LHP, it will typically take several hours for the loop to reach a new steady state when the CC temperature (saturation temperature) was not actively controlled. The reason is that although the CC temperature governs the loop saturation temperature, its own temperature is subjected to changes of the pump power, condenser temperature, and thermal capacitance of the heat source. In this CLHP test, the CLHP could usually reach a steady state within an hour after a power change because of the following reasons: 1) the copper evaporator plate has a very low thermal capacity due to its extremely low specific heat. It also had an extremely large thermal conductivity to yield a uniform temperature over the entire evaporator plate. 2) The capillary pump wick was made of stainless steel which had a very small thermal conductivity, leading to very little heat leak from the pump to the CC. 3) The CC itself worked as a condenser and there was no liquid line whose temperature could be further affected by the ambient temperature. Once T_{CC} was settled, temperatures of the rest of the loop reached steady temperatures quickly.

In Figure 11, the loop started with Q_{PUMP}/Q_{EVAP} of 20mW/0mW. After the loop reached a steady state, the difference between T_{PUMP} and T_{SAT} was 0.75K, and the difference between T_{EVAP} and T_{SAT} was 0.2K. In subsequent power changes, the following general trend was observed: 1) When Q_{EVAP} increased and Q_{PUMP} remained unchanged, T_{COND} and T_{CC} increased because more heat was dissipated by the condenser and the CC (which worked as part of the condenser). Consequently, T_{SAT} increased, leading to the increase of T_{EVAP} and T_{PUMP}. The difference between T_{PUMP} and T_{SAT} was unchanged because Q_{PUMP} was unchanged. On the other hand, the difference between T_{EVAP} and T_{SAT} increased due to the increase of Q_{EVAP}. 2) When Q_{PUMP} increased and Q_{EVAP} remained unchanged, T_{COND} and T_{CC} increased because more heat was dissipated by the condenser and CC. This led to the increase of

T_{SAT}, T_{EVAP} and T_{PUMP}. The difference between T_{PUMP} and T_{SAT} increased due to an increase of Q_{PUMP}. The difference between T_{EVAP} and T_{SAT} remained unchanged or decreased slightly because Q_{EVAP} was unchanged but the rate of flow circulation increased. This test also verified that the evaporator could remove twice as much power as that applied to the pump for Q_{PUMP} between 20 mW and 60 mW.

Note that a change in Q_{PUMP} and/or Q_{EVAP} could result in changes in the fluid composition (subcooled liquid, two-phase fluid, and superheated vapor) along the evaporator line and the underlying heat transfer processes. This led to changes in T_{COND}, T_{SAT}, T_{PUMP}, and T_{EVAP}. However, the uniform temperature of the evaporator plate due to a high thermal conductivity of copper made it impossible to verify experimentally the change of fluid composition along the evaporator line.

Figure 12 presents temperature profiles of another power ramp-up test. The loop started with Q_{PUMP}/Q_{EVAP} of 20mW/20mW. The power then changed to 30mW/60mW, 40mW/80mW, and 50mW/100mW. Again, the loop could reach a new steady state quickly, and the evaporator was able to dissipate twice as much power as that applied to the pump for Q_{PUMP} between 20 mW and 50 mW.

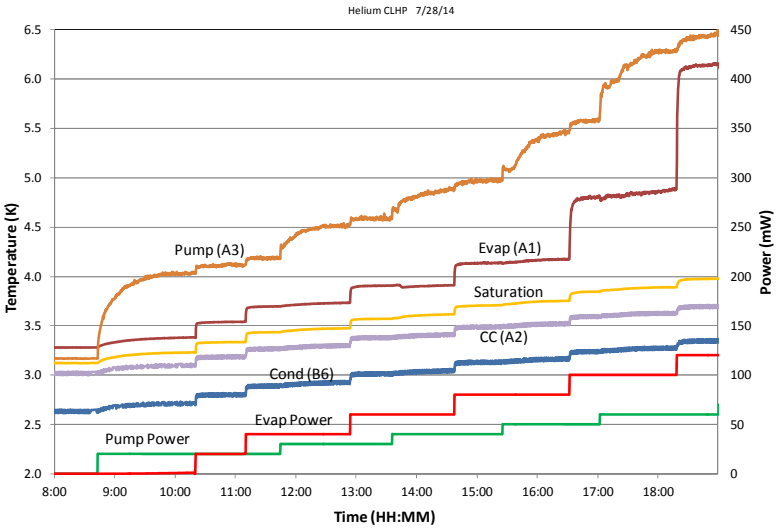

Figure 11. Power Ramp-up Test

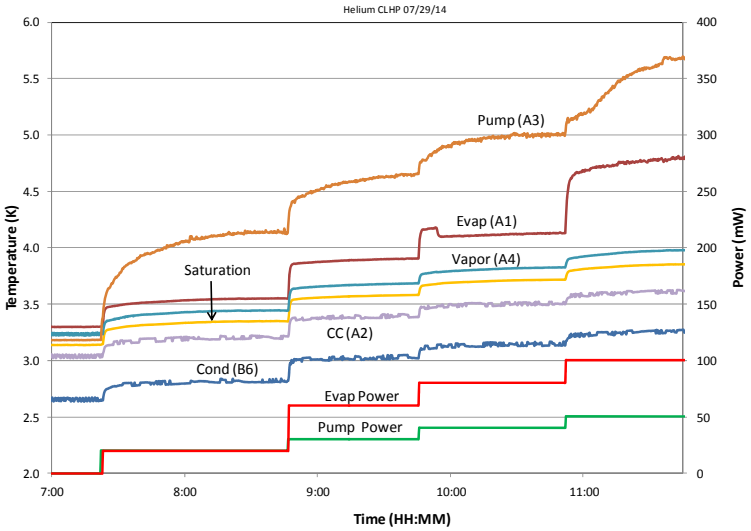

Figure 12. Power Ramp-up Test

D. Power Cycle

The purpose of the power cycle test was to investigate the ability of the loop to adapt to a rapid and large change of the evaporator heat load. Figure 13 illustrates the loop temperatures during a power cycle test with Q_{PUMP}/Q_{EVAP} varied from 50mW/100mW to 50mW/20mW, and then back to 50mW/100mW. With an evaporator power turn down ratio of 5, the loop demonstrated its ability to adapt to a rapid change of power to the evaporator and quickly reached a new steady state. Moreover, the temperature profiles at Q_{EVAP} of 100 mW were essentially the same before and after the power change. When Q_{EVAP} changed from 100 mW to 20 mW, T_{EVAP} decreased from 4.8K to 3.7K.

The sudden decrease of evaporator power did cause some fast transients in loop temperatures. As Q_{EVAP} decreased from 100 mW to 20 mW, T_{COND}, T_{CC}, and T_{SAT} all decreased rapidly. The corresponding saturation pressure in the loop also decrease quickly. A decrease in the system pressure means that the hot reservoir contains less vapor and the excess vapor was injected into the CLHP. The injection of warm vapor into the CLHP was evidenced by the sharp rise of temperatures at the CC inlet (A5) and evaporator outlet (B5) as shown in Figure 14. After a few minutes, all transients diminished and the loop operated stably.

Another power cycle test was conducted with Q_{PUMP}/Q_{EVAP} varying from 40mW/80mW to 40mW/20mW, and then back to 40mW/80mW. Again, the loop was able accommodate a rapid change of power to the evaporator and quickly reached a new steady state. The temperature profiles at Q_{EVAP} of 80 mW were the same before and after the power change. Fast temperature transients also occurred when Q_{EVAP} changed from 80 mW to 20 mW, as shown in Figure 15. Because of a smaller absolute power change and a smaller power turn down ratio in this test, changes in the loop temperatures during the transient were smaller than those shown in Figure 14, and the transients diminished more quickly.

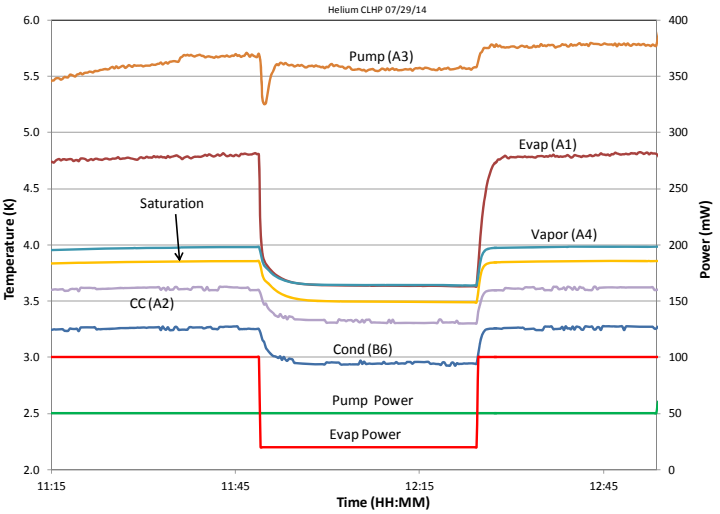

Figure 13. Power Cycle Test

E. Pump Capillary Limit

The capillary limit of the pump governs the maximum flow rate that can be circulated through the loop, which ultimately determines the maximum evaporator heat removal capability. In the traditional LHP test, the capillary limit can be found by continuing to increase the pump power until the capillary limit is exceeded, which is caused by vapor blowing through the wick and manifested by a rapid increase of the CC temperature and the rise of the liquid line temperature to near the CC temperature.

In the CLHP tested under this program, there is no liquid line and the CC works as part of the condenser. When the pump capillary limit is exceeded, some vapor will penetrate trough the primary wick and flow to the CC. However, because the CC also works as a condenser, the CC or saturation temperature will not be much affected. A good way to find the pump capillary limit is to apply a constant power to the evaporator and then keep increasing the pump power. When the capillary limit is exceed, some vapor will penetrate the wick and the forward fluid flow to the evaporator will decrease. This will lead

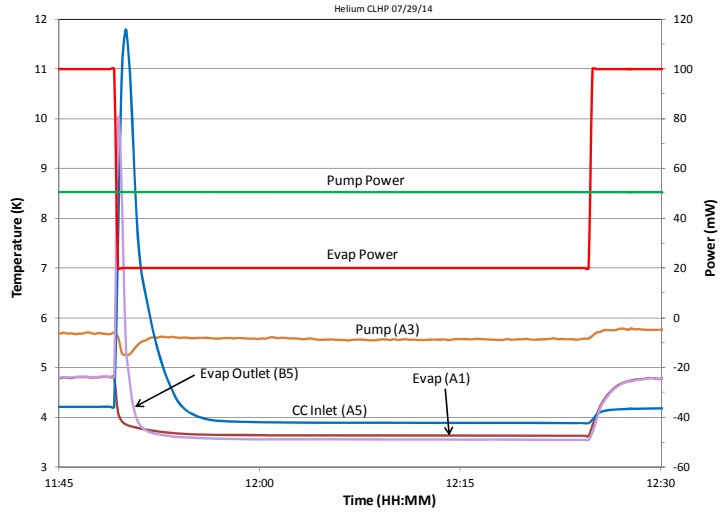

Figure 14. Temperature Transients during Power Cycle Test

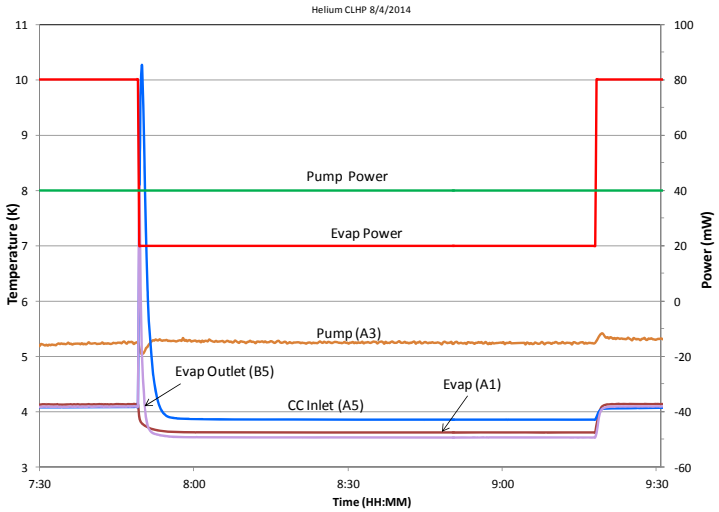

Figure 15. Temperature Transients during Power Cycle Test

to an increase in the difference between the evaporator temperature and the loop saturation temperature. Moreover, unlike the traditional LHP, the current CLHP can have independent heat loads to the pump and evaporator. Thus, the capillary limit must be expressed in terms of a combination of Q_{PUMP} and Q_{EVAP}. Hence the above-mentioned method of finding the capillary limit will yield a capillary limit, which is not the only capillary limit. When Q_{EVAP} changes, a new Q_{PUMP} can be found to cause the pump to exceed its capillary limit.

Figure 16 shows loop temperature profiles during a capillary limit test where Q_{EVAP} was kept constant at 100 mW while Q_{PUMP} increased gradually from 50 mW to 90 mW with increments of 10 mW. It was inferred from T_{EVAP} that the pump reached its capillary limit when Q_{PUMP}/Q_{EVAP} was between 80mW/100mW and 90mW/100mW.

The same capillary limit test was repeated and the temperature profiles are shown in Figure 17. The result was consistent with that shown in Figure 16, i.e. the pump capillary limit was reached at Q_{PUMP}/Q_{EVAP} between 80mW/100mW and 90mW/100mW. The loop recovered quickly when the pump power was reduced to 60mW.

F. Steady State Operation

Several tests were conducted to demonstrate the long term operation of the CLHP for Q_{PUMP}/Q_{EVAP} of 50 mW/100 mW, 40 mW/80 mW, 30 mW/60 mW, 30 mW/45 mW, 20 mW/40 mW, and 10 mW/20 mW, respectively. The test duration ranged from 10.5 hours to 17 hours. In all tests, the loop operated stably and all temperatures remained essentially unchanged for the entire test period.

Figure 18 depicts the temperature profiles during the 11-hour steady state operation with Q_{PUMP}/Q_{EVAP} at 50mW/ 100mW. This test illustrated the loop steady state operation at high powers. For low powers, long duration steady state operation with Q_{PUMP}/Q_{EVAP} of 10mW/20mW was also successfully demonstrated for 10.5 hours.

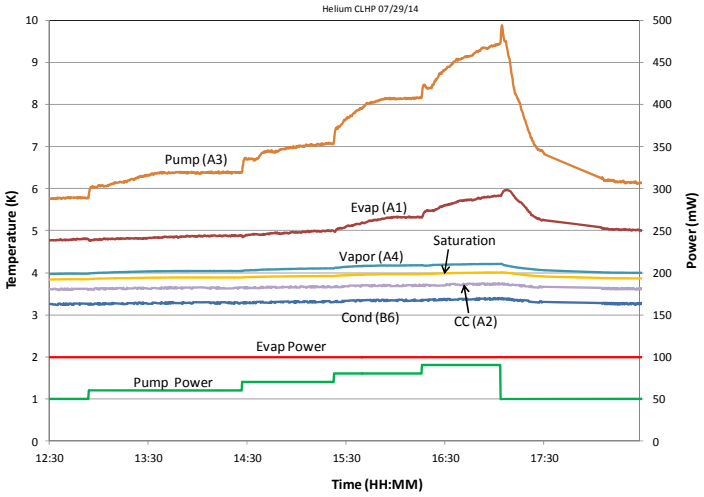

Figure 16. Pump Capillary Limit Test

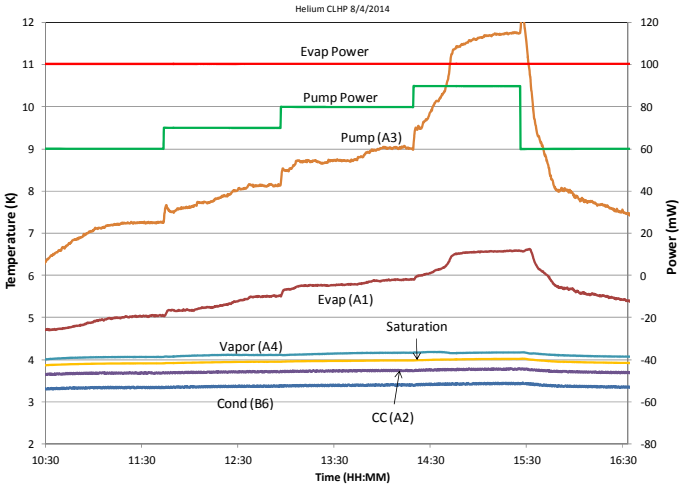

Figure 17. Pump Capillary Limit Test

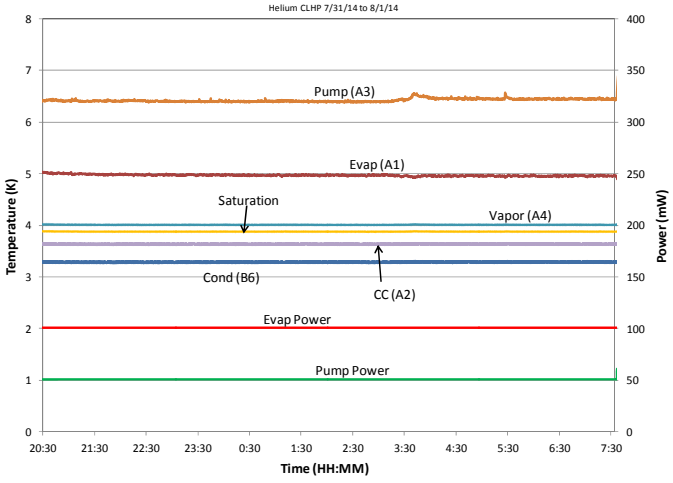

Figure 18. Steady State Operation at Q_{PUMP}/Q_{EVAP} of 50mW/100mW

Over one weekend, the CLHP was undergoing steady state operation continuously for 58 hours at various combinations of Q_{PUMP}/Q_{EVAP}. Figure 19 shows temperature profiles for the 10.5-hour operation with Q_{PUMP}/Q_{EVAP} of 30mW/60mW. This test was proceeded by operation with Q_{PUMP}/Q_{EVAP} of 40mW/80mW for 17 hours, and followed by operation with Q_{PUMP}/Q_{EVAP} of 30mW/45 mW for 15 hours. It is seen that the loop temperatures were very stable and transitions from one power setting to the next were very smooth.

G. Evaporator Heat Removal Capability

The analysis presented in Section 2 states that, assuming the fluid flow enters the evaporator as saturated liquid and leaves as saturated vapor, the maximum heat that can be removed by the evaporator will be no more than the heat applied to the capillary pump multiplied by the number of loopbacks in the evaporator plate. The CLHP being tested has two loop backs, and hence, the ratio of Q_{EVAP} to Q_{PUMP} for this loop should be 2 or less.

The evaporator heat removal capability tests were conducted with Q_{PUMP} = 10 mW, 20 mW, 30 mW, 40 mW, and 50 mW. In each case, the ratio of Q_{EVAP} to Q_{PUMP} was higher than 2, and could be as high as 4 for Q_{PUMP} of 10 mW and 20 mW. Similar results of evaporator heat removal capability higher than twice the pump power were obtained in the previous neon LHP test [7]. This was puzzling.

One possibility was an error in the measurement of Q_{PUMP} and Q_{EVAP}. Both powers were obtained using 4-wire measurements, which measured the voltage directly across the heaters excluding the line voltage drops. In addition, other instruments were used to verify the heater resistance, voltages and currents. All measurements yielded the same results as displayed by the Labview software. Hence, the power values should be correct.

Another possibility was that the flow could enter the evaporator as subcooled liquid and leave the evaporator as superheated vapor when the ratio of Q_{EVAP} to Q_{PUMP} exceeded 2. Experimental results of the helium CLHP temperatures strongly suggest such a possibility.

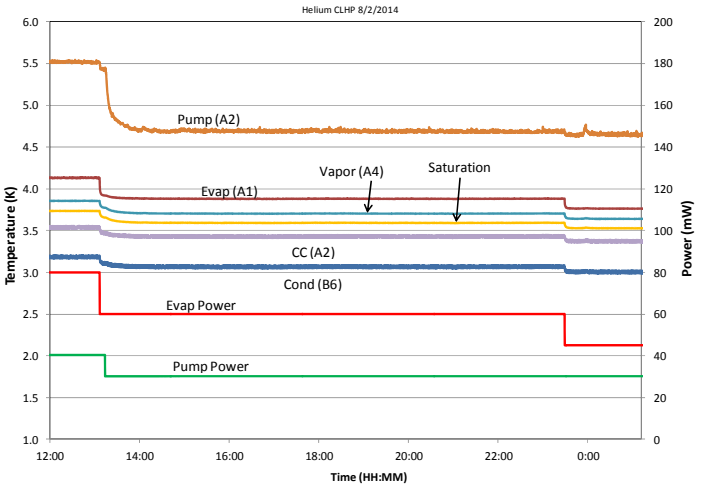

Figure 19. Steady State Operation at Q_{PUMP}/Q_{EVAP} of 30mW/60mW

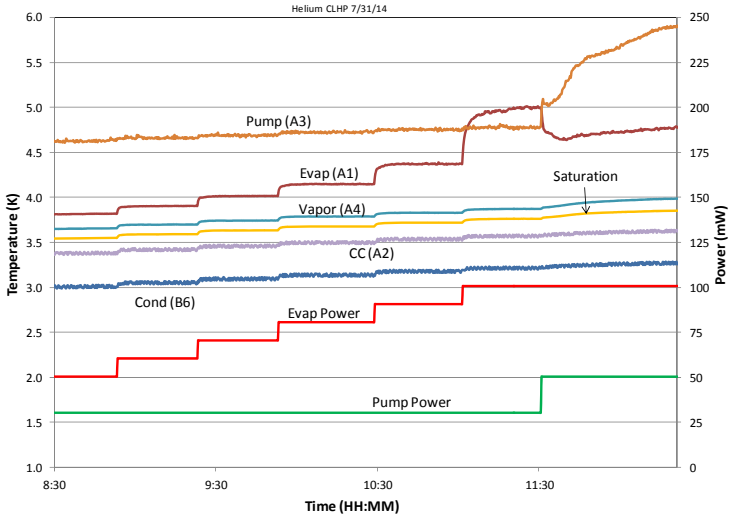

Figure 20. Evaporator Heat Removal with 30mW to Pump

Figure 20 shows results of an evaporator heat removal capability test with a constant Q_{PUMP} = 30 mW, and Q_{EVAP} increased from 50 mW to 100 mW with 10 mW increments. For each 10 mW increment of Q_{EVAP}, T_{SAT} increased about the same amount, and T_{PUMP} followed accordingly. On the other hand, T_{EVAP} showed a larger increase because of heat transfer requirement. From Q_{EVAP} = 50 mW to Q_{EVAP} = 80 mW, T_{EVAP} increased about the same amount at each change, indicating a rather constant thermal conductance. At Q_{EVAP} = 90 mW, T_{EVAP} began to increase by a larger amount, and at Q_{EVAP} = 100 mW, T_{EVAP} had a large jump. This indicated a decrease in the thermal conductance, possibly due to a deviation from the two-phase liquid evaporation within the evaporator. Moreover, when Q_{PUMP} increased from 30 mW to 50 mW, T_{EVAP} dropped quickly although T_{SAT} increased. If at

Q_{PUMP}/Q_{EVAP} of 50mW/100mW heat is transferred by two-phase inside the evaporator, then at Q_{PUMP}/Q_{EVAP} of 30 mW/100 mW heat could not be transferred entirely by liquid evaporation. In other words, single-phase (liquid and/or vapor) heat transfer must also be involved. Heat transfer from the evaporator to the fluid vapor at Q_{PUMP}/Q_{EVAP} of 30 mW/100 mW could occur. From the user's point of view, heat was still be removed, but at the expense of a higher evaporator temperature.

The evaporator heat removal test continued with Q_{PUMP} = 50 mW. Figure 21 shows that the pump temperature was steady at 6K, similar to that shown in Figure 18 for steady long duration operation. Following the same argument, one can infer that from Q_{EVAP} = 100 mW to Q_{EVAP} = 130 mW, the thermal conductance was more or less constant. When Q_{EVAP} increased to 140 mW, however, the thermal conductance decreased appreciably, indicating some single-phase heat transfer occurred inside the evaporator. Unfortunately, it was not possible to confirm exactly when the transition occurred because all temperature sensors on the evaporator plate (A1, B7, and B8) exhibited the same temperature due to the extremely high thermal conductivity of copper.

The contribution of liquid subcooling and vapor superheat can be estimated under the ideal condition. The wick in the capillary pump was made of stainless steel, which had a very low thermal conductivity at low temperatures. The heat leak from the capillary pump to the CC was therefore near zero. The CC also served as the condenser and there was no liquid subcooling to the CC. Thus, the effectiveness of the capillary pump, η in Equation (1), was equal to unity under such an ideal case. The cryocooler second stage had a cooling capacity of more than 1W at 4K. The vapor generated in the capillary pump could be completely condensed in the condenser and become subcooled before entering the evaporator. The liquid could be completely vaporized and become superheat vapor when exiting the evaporator. The amount of liquid subcooling can be calculated as $\dot{m}C_{p,l}\Delta T_{SUB}$, where $\dot{m}$ is mass flow rate, $C_{p,l}$ is liquid specific heat, and ΔT_{SUB} is the difference between T_{SAT} and T_{COND}. Likewise, the contribution from the superheat vapor can be calculated as $\dot{m}C_{p,v}\Delta T_{SUP}$, where $C_{p,v}$ is vapor specific heat, and ΔT_{SUP} is the difference between the T_{EVAP} and T_{SAT}. Thus, the additional heat removed by the evaporator due to single-phase heat transfer can be calculated approximately by:

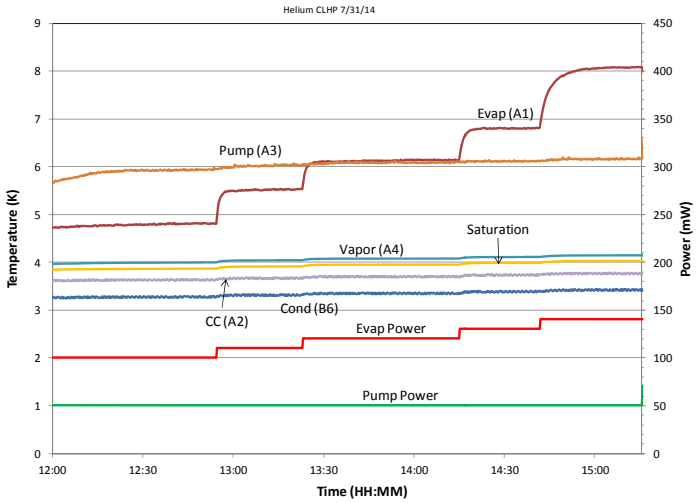

Figure 21. Evaporator Heat Removal with 50 mW to Pump

Table 2. Maximum Heat Removal by Evaporator

Q_{PUMP} (mW)	Experimental data of Q_{EVAP} (mW)	Q^*_{EVAP} calculated by Eq. (6) (mW)
20	80	50
30	90	78
40	100	102
50	140	183

$$Q_{EVAP,\,S} = 2(Q_{PUMP}/\lambda)[C_{p,l}(\,T_{SAT} - T_{COND}\,) + C_{p,v}\,(T_{EVAP} - T_{SAT}.)] \qquad (5)$$

And the total heat that the evaporator can remove becomes:

$$Q^*_{EVAP} = 2\,Q_{PUMP} + Q_{EVAP,\,S} \qquad (6)$$

The test data of Q_{EVAP} and the amount of heat calculated from Eq. (6) for a given Q_{PUMP} are shown in Table 2, where the temperature-dependent fluid properties were included in the calculations. It is seen that single-phase heat transfer could add an additional 25 to 30 percent to the two-phase heat transfer. Compared to the test data, Eq. (6) underestimates the evaporator heat removal at Q_{PUMP} = 20mW and over estimates the heat removal at Q_{PUMP} = 50mW by a large percentage.

There could be other heat loss from the evaporator plate that was not identified or other physical processes involved in the evaporator heat removal that are still not understood.

V. Summary and Conclusions

Extensive tests of the helium CLHP were conducted to characterize its steady state and transient behaviors. Tests conducted included loop cool-down from the ambient temperature, startup, low power operation, power cycle, pump capillary limit, evaporator heat removal capability, and long duration steady state operation. The helium CLHP demonstrated reliable operation and robust performance. Test results clearly verified the ability of the helium CLHP to cool large areas or components where heat was collected from a large area and dissipated to a cryocooler. The loop could be cooled from the ambient temperature to subcritical temperature very effectively, and start successfully by applying power to both the capillary pump and evaporator without the need of any pre-conditioning such as pressure priming. When the pump power and/or evaporator power changed, the loop could adapt to changes and reach a new steady state very quickly. The evaporator could remove heat loads between 10 mW and 140 mW with a turn down ratio of 14. When the heat input exceeded the maximum heat removal capability of the evaporator, the evaporator temperature would rise, but could resume its normal function by reducing the evaporator heat input or increasing the power to the capillary pump. Several tests were conducted to demonstrate the steady state operation of the CLHP with durations up to 17 hours.

Acknowledgments

Funding for this test program was provided by NASA Engineering and Safety Center's Passive Thermal and Propulsion Technical Discipline Teams. The Technical Monitors were Messrs Steven Rickman and the late Roberto Garcia. Thanks also go to Dr. Triem Hoang and Ms. Tamara O'Connell for their valuable advices during the course of this investigation.

References

1. Goncharov, K., Nikitkin, M., Fershtater, Y., and Maidanik, Y., "Loop Heat Pipes in Thermal Control System for OBZOR Spacecraft, 25th *International Conference on Environmental Systems*, San Diego, California, July 10-13, 1995.
2. Grob, E., Baker, C., and McCarthy, T., "Geoscience Laser Altimeter System (GLAS) Loop Heat Pipe: An Eventful First Year On-Orbit", Paper No. 2004-01-2558, *34th International Conference on Environmental Systems*, Colorado Springs, Colorado, July 19-22, 2004.
3. Grob, E., "Performance of the GLAS Loop Heat Pipes – 7 Years in Orbit", Paper No. AIAA-2010-6029, *40th International Conference on Environmental Systems*, Barcelona, Spain, July 11-15, 2010.
4. Choi, M., "Thermal Assessment of Swift Instrument Module Thermal Control System during First 2.5 Years in Flight," Paper No. 2007-01-3083, *37th International Conference on Environmental Systems*, Chicago, Illinois, July 9-12, 2007.
5. Rodriguez, J. I., Na-Nakornpanom, A., Rivera, J., Mireles, V. and Tseng, H., "On-Orbit Thermal Performance of the TES Instrument – Three Years in Space," SAE Paper No. 2008-01-2118, *38th International Conference on Environmental Systems*, San Francisco, California June 30 - July 2, 2008.
6. Nikitkin, M. and Wolf, D., "Development of LHP with Low Control Power," Paper No. 2007-01-3237, *37th International Conference on Environmental Systems*, Chicago, Illinois, July 9-12, 2007.
7. Ku, J. and Robinson, F., "Testing of a Neon Loop Heat Pipe for Large Area Cryocooling," Paper No. ICES 2014-35, *44th International Conference on Environmental Systems*, Tucson, Arizona, July 13-17, 2014.
8. Maidanik, Y., and Fershtater, Y., "Theoretical Basis and Classification of Loop Heat Pipes and Capillary Pumped Loops," *10th International Heat Pipe Conference*, Stuttgart, Germany, 1997.
9. Ku, J., "Operating Characteristics of Loop Heat Pipes," Paper No. 1999-01-2007, *29th International Conference on Environmental Systems*, Denver, Colorado, July 12-15, 1999.
10. Maidanik, Y., "Loop Heat Pipes – Theory, Experimental Developments and Application," *13th International Heat Pipe Conference*, Sydney, Australia, August 9-13, 2006.
11. Ku, J., "Heat Load Sharing in a Loop Heat Pipe with Multiple Evaporators and Multiple Condensers," Paper No. AIAA-2006-3108, *9th AIAA/ASME Joint Themophysics and Heat Transfer Conference*, San Francisco, CA, June 5-8, 2006.
12. Hoang, T., O'Connell, T.A., Khrustalev, D., and Ku, J, "Cryogenic Advanced Loop Heat Pipe in Temperature Range of 20-30 K," *12th International Heat Pipe Conference*, May 19-24, 2002, Moscow, Russia.
13. Hoang, T., O'Connell, T., Ku, J., Butler, B. and Swanson, T., "Large Area Cryocooling for Far Infrared Telescopes," Paper No. AM125-8, *International Symposium on Optical Science and Technology, SPIE's 48th Annual Meeting*, August 3-8, 2003, San Diego, California.
14. Hoang, T., O'Connell, Sukhov, D., and Ku, J., "Large -Area Cooling with Cryogenic Loop Heat Pipes," Paper No. AIAA-2007-4272, *39th AIAA Thermophysics Conference*, Miami, Florida, June 25-28, 2007.
15. Maidanik, Y. F., Solodovnik, N. N., and Fershtater, Y. G., "Investigation of Dynamic and Stationary Characteristics of a Loop Heat Pipe," *IX International Heat Pipe Conference*, Albuquerque, New Mexico, May 1-5, 1995.
16. Ku, J., Ottenstein, L., Rogers, P., and Cheung, K., "Investigation of Low Power Operation in a Loop Heat Pipe," SAE Paper No. 2001-01-2192, *31st International Conference on Environmental Systems*, Orlando, Florida, July 9-12, 2001.